

Nucleation and early stage crystallization in barium disilicate glass

Ling Cai, Randall E. Youngman, David E. Baker, Aram Rezikyan, Minghui Zhang, Bryan Wheaton, Indrajit Dutta, and Bruce G. Aitken
Science and Technology Division, Corning Incorporated, Corning, NY, USA

Andrew J. Allen
*Materials Measurement Science Division,
National Institute of Standards and Technology, Gaithersburg, MD, USA*

Abstract

Barium disilicate is one of the glass-ceramic systems where internal nucleation and crystallization can occur from quenched glass upon heat treatment without requiring nucleating agents. The structural origin of the nano-clusters formed during low temperature heat treatment is of great interest in gaining a fundamental understanding of nucleation kinetics in silicate glasses. Here, we present experimental investigations on the low temperature heat treatment of barium disilicate ($\text{BaO} \cdot 2\text{SiO}_2$) glass. Several experimental techniques were used to characterize the structural nature of barium disilicate glasses that were heat treated between the glass transition temperature, T_g , and the peak temperature of crystal growth, T_{cr} . The data show that small amounts of crystallites including BaSi_2O_5 as well as other higher Ba/Si ratio phases are formed. Moreover, unlike that reported for lower BaO content ($\text{BaO} < 33\text{mol}\%$) barium silicate glass or the analogous $\text{Li}_2\text{O}-\text{SiO}_2$ glasses, no clear evidence is observed for liquid/liquid phase separation in barium disilicate glass.

Keywords: silicate glass; nucleation in glass; small angle scattering;

I. INTRODUCTION

The growth of crystals inside amorphous silicate glasses by heat treatment has been utilized to make glass-ceramics that are integrated into products for everyday life and technological applications [1, 2, 3, 4]. Although glass-ceramic technology has been developed for more than fifty years, there remain unanswered questions regarding the nucleation process. For example, does the glass become phase separated upon heat treatment from the as-quenched state, and how does the glass chemical composition determine the homogeneous or heterogeneous nature of the nucleation process? The answers to these questions are critical for future development of glass-ceramics where the physical properties (e.g. refractive index, thermal expansion coefficient, fracture toughness) are dependent on the glass composition and heat treatment schedule [5, 6, 7].

A prototypical system for the study of nucleation in glass is that of the binary barium silicates. Certain glass compositions in this system, when heat treated, spontaneously nucleate without the need of a nucleating agent. Yet the phase diagram indicates that small changes in Ba/Si ratio can introduce significant differences in the phase morphology and crystalline structure after heat treatment [8, 9, 10, 11, 12, 13, 14, 15]. Among the barium silicate compositions, barium disilicate (BaO_2SiO_2) has been extensively studied recently because of new evidence suggesting an apparent deviation from the previously postulated homogeneous nucleation process [16, 17, 18]. The immiscibility phase diagram for barium disilicate glass suggests that the barium disilicate glass is right on the border of phase separation, and once fully crystallized the main phase is BaSi_2O_5 (BS2) while other higher Ba/Si ratio crystalline phases such as $\text{Ba}_2\text{Si}_3\text{O}_8$ (B2S3), $\text{Ba}_3\text{Si}_5\text{O}_{13}$ (B3S5), and $\text{Ba}_5\text{Si}_8\text{O}_{21}$ (B5S8) are also present [9]. For a system that has the same Ba/Si ratio in both the amorphous and crystalline phase, and containing no nucleating agent, homogenous nucleation seemed to be a likely mechanism. But new evidences have shown that, not only does the BS2 phase split into two polymorphs [19], small amounts of higher Ba/Si ratio crystalline phases such

as $\text{Ba}_2\text{Si}_3\text{O}_8$ (B2S3), $\text{Ba}_3\text{Si}_5\text{O}_{13}$ (B3S5), and $\text{Ba}_5\text{Si}_8\text{O}_{21}$ (B5S8) are also found during the growth stage or earlier [17]. Moreover, a recent theoretical study has also concluded that B5S8 crystalline clusters have more positive solvation energy than that of barium disilicate clusters, which suggests local regions of B5S8 stoichiometry could have formed at the initial stages of nucleation [20]. Therefore, it is important to revisit the barium disilicate system to investigate whether there is any further evidence at the nucleation and early crystallization stages that supports a heterogeneous nucleation mechanism.

In this work we present an experimental study of barium disilicate glasses that are heat treated at temperatures well below the peak of crystal growth but just slightly above the glass transition for different periods of time. We use complementary techniques such as x-ray diffraction (XRD), scanning electron microscopy (SEM), transmission electron microscopy (TEM), nuclear magnetic resonance (NMR) and synchrotron small angle x-ray scattering (SAXS) to understand the structural changes in nano clusters that transition from amorphous to early stage crystallization.

II. EXPERIMENTAL

The barium disilicate glass was made using a 2500 g batch of barium carbonate and high-purity silica, mixed in the proper proportion and melted in a covered platinum crucible at 1600 °C for 6 h. The liquid was roller-quenched, the resulting solid broken into smaller pieces, and then re-melted at 1500 °C for 6 h. A homogenous glass was obtained by pouring the melt onto a stainless steel table. Samples for this nucleation study were taken from this quenched (unannealed) glass. The barium disilicate glass composition was confirmed using inductively-coupled plasma–optical emission spectroscopy (ICP-OES). The glass transition and crystallization temperatures, T_g and T_{cr} , were estimated from differential scanning calorimetry (DSC).

^{29}Si solid-state NMR spectroscopy was performed at 4.7 and 11.7 T magnetic field strengths (39.69 and 99.28 MHz resonance frequency, respectively) using Agilent DD2 consoles (Agilent Technologies*, CA) and Agilent/Varian 9.5 or 5 mm magic angle spinning (MAS) NMR probes (Agilent Technologies, CA). Unannealed and heat-treated glass samples were powdered with an agate mortar and pestle, and packed into 9.5 or 5 mm outer diameter zirconia rotors for NMR studies at 3 or 8 kHz sample spinning rates, respectively. Direct polarization spectra were acquired with a $\pi/6$ pulse width of 2.4 μs , a recycle delay of 300 s and acquisition of 340 to 580 scans. ^{29}Si NMR data were frequency referenced to tetramethylsilane at 0.0 ppm and processed with Gaussian apodization of 25 Hz. NMR spectra were processed with VnmrJ software (Agilent Technologies, CA), and plotted and fitted using DMFit [21].

Samples for SEM analyses were prepared as fractured cross-sections followed by a 10 second, 0.1% HF acid etch and deionized (DI) water rinse. The etched and rinsed samples were then coated with conductive carbon and analyzed using a Zeiss 1550VP Field Emission SEM (FESEM) (Carl Zeiss Microscopy LLC, Thornwood, NY) operated at 5 kV accelerating potential and 150 pA beam current. The lower beam energy decreases the landing energy of the analysis beam, increasing resolution and enhancing surface sensitivity. Secondary electron images were acquired at 1024×768 pixels with horizontal field widths as small as 1130 nm to analyze the glass matrix and crystal microstructure.

High temperature X-ray diffraction (HTXRD) was performed utilizing a PANalytical XPert powder diffraction system (Malvern Panalytical Inc., Westborough, MA) equipped with an Anton Paar HTK1200N furnace and an XCeerator detector (Anton Paar GmbH, Graz, Austria). The

* Certain commercial instruments, materials, or processes are identified in this paper to adequately specify the experimental procedure. Such identification does not imply recommendation or endorsement by the National Institute of Standards and Technology, nor does it imply that the instruments, materials, or processes identified are necessarily the best available for the purpose.

temperature of the diffraction furnace was carefully calibrated through a series of melting point and phase change standards. Barium disilicate glass was ground with a mortar and pestle into a fine powder and packed into standard HTXRD alumina crucibles. The HTXRD measurement was a step or staircase profile with a 10°C/min heating rate and 30 min holds for collection of two, 15-min diffraction scans, every 50°C between 600°C and 1100°C.

Synchrotron X-ray scattering experiments were performed at the ultra-small-angle X-ray scattering (USAXS) beamline, sector 9-ID, of the Advanced Photon Source (APS), Argonne National Laboratory, Argonne, IL. Melt-quenched barium disilicate samples were made into 7 mm diameter and 0.25 mm thick coupons. An X-ray energy of 21 keV was selected for the experiment. For room temperature measurements, the samples were mounted on a multi-position sample paddle for automated measurements. For each high-temperature in-situ measurement, the disk sample was placed inside the Linkam 1500 heater, where a heating rate of 200°C/min can be achieved. At each measurement, ultra-small-angle, small-angle and wide-angle X-ray scattering (USAXS, SAXS, and WAXS) data were collected sequentially, with each combined USAXS/SAXS/WAXS scan taking about 6 minutes. The X-ray beam size on the sample was 0.8 mm × 0.8 mm for USAXS, and 0.8 mm horizontal x 0.2 mm vertical for SAXS and WAXS. The USAXS/SAXS/WAXS measurements provided fully-calibrated scattering intensity data versus Q (where $Q = (4\pi/\lambda)\sin(\theta)$, λ is the X-ray wavelength (0.5904 Å for 21 keV X-rays) and θ is one-half of the scattering angle. The Q -ranges covered were $0.0001 \text{ \AA}^{-1} < Q < 0.3 \text{ \AA}^{-1}$ for USAXS, $0.05 \text{ \AA}^{-1} < Q < 1.7 \text{ \AA}^{-1}$ for SAXS, and $1.4 \text{ \AA}^{-1} < Q < 6.3 \text{ \AA}^{-1}$ for WAXS (XRD) measurements, although the WAXS maximum Q was constrained to $\approx 4.5 \text{ \AA}^{-1}$ for measurements in the Linkam heater. Full details of the APS USAXS facility can be found elsewhere [22].

TEM data were collected using an aberration corrected FEI Titan instrument operated at 200

keV electron beam energy. High-resolution bright-field electron micrographs from barium silicate crystals were recorded in the scanning mode (STEM). Barium silicate crystals are easily damaged by high energy electrons; therefore, exposure was minimized when possible. A large number of crystals were imaged to find those oriented along a high-symmetry zone axis. Selected area electron diffraction (SAED) patterns were recorded by a Gatan Orius retractable CCD camera, Model 833.P76N (Gatan Inc., Pleasanton, CA) using 10 μm SA aperture equivalent to about 150 nm on the sample.

TEM samples were initially prepared by in-situ liftout inside a FEI Quanta 3D 600 dual beam FIB/SEM instrument (30 keV Ga-ion beam), including the one from which SAED data shown below were obtained. Thinning beyond about 150 nm was done using a 5 keV beam energy with a final 2 keV polishing step in order to minimize crystal amorphization. Samples for high-resolution STEM imaging were prepared by the conventional TEM preparation method (polishing, dimpling, followed by Ar-ion milling with precision ion polishing (PIPS)). This method allowed for preparation of a larger electron-transparent area in order to maximize the probability of finding zone-axis-oriented crystals, especially if the number density of crystals is low.

III. RESULTS

Thermal analysis on the parent barium silicate glass with 33.3 mol% of BaO (analyzed) indicates that the glass transition temperature, T_g , is around 690°C, and an exothermic peak corresponding to the crystallization temperature, T_{cr} , is at $\approx 840^\circ\text{C}$, see **Figure 1**. The value for T_{cr} is in accordance with those measured for a broader range of BxSy glass compositions [23]. Note the second exotherm at $\approx 960^\circ\text{C}$ is related to the morphological transformation of BS2 phase [24, 25, 26]. With these characteristic temperatures for the barium disilicate glass determined, the subsequent study focused on extensive heat treatments of the glass between $T_g = 690^\circ\text{C}$

and $T_{cr} = 840^{\circ}\text{C}$ to investigate early stage nucleation phenomena.

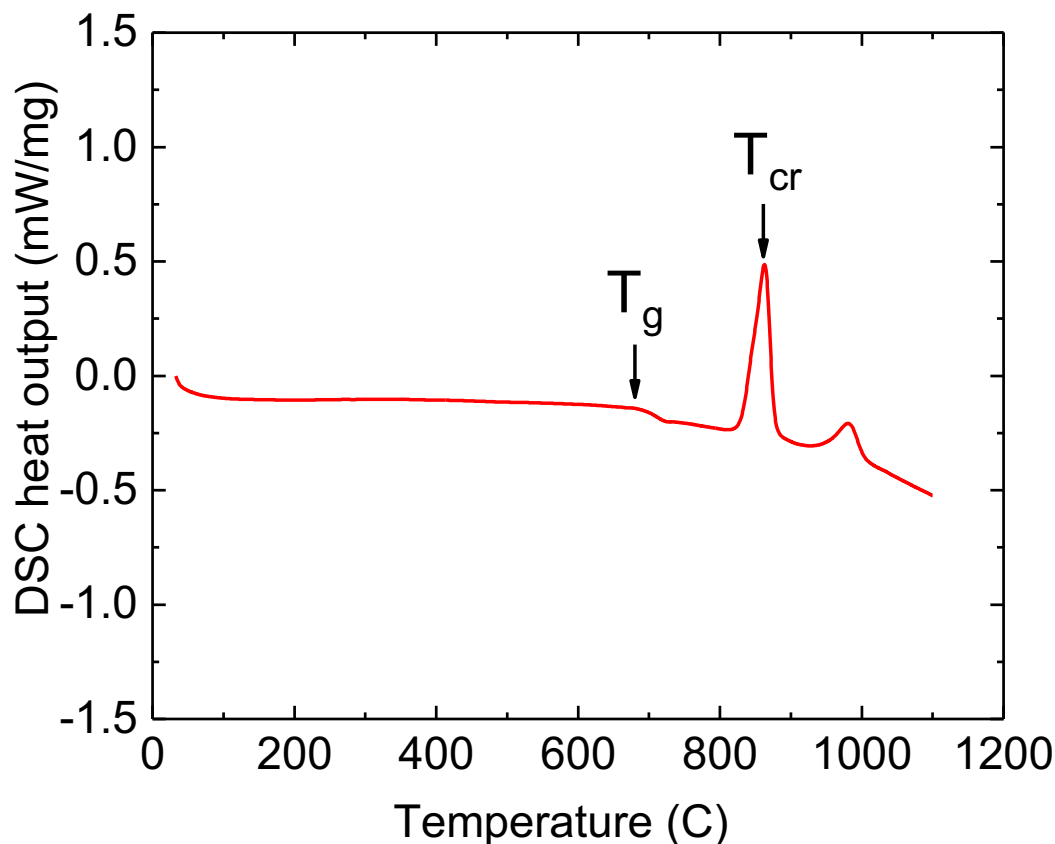


Figure 1 DSC scan for barium disilicate glass. The glass transition endotherm (T_g), as well as the crystallization exotherm (T_{CR}), are labeled.

In the high temperature in-situ XRD measurement, diffraction peaks were not detected until the sample reached $\approx 800^{\circ}\text{C}$, as shown in **Figure 2a**, suggesting that crystallization begins between 750 and 800°C . The diffraction pattern of the barium disilicate sample at this temperature predominately matched that of the BS2 phase, which corresponds to the first crystallization peak in DSC, at approximately 840°C [27, 28]. However, diffraction peaks corresponding to higher Ba/Si ratio phases are also present, and they are particularly evident at low diffraction angle, see **Figure 2b**. Interestingly, at higher temperature, the BS2 phase grows rapidly while the diffraction

intensity of the higher Ba/Si phases diminishes, see **Figure 2c**. This is particularly evident on the B3S5 peak at around 23°, where the intensity is strong at 800°C but much weaker at 950°C. Nevertheless, the strong growth of the BS2 phase may have led many previous studies to conclude that barium disilicate glass undergoes homogeneous nucleation [26, 18].

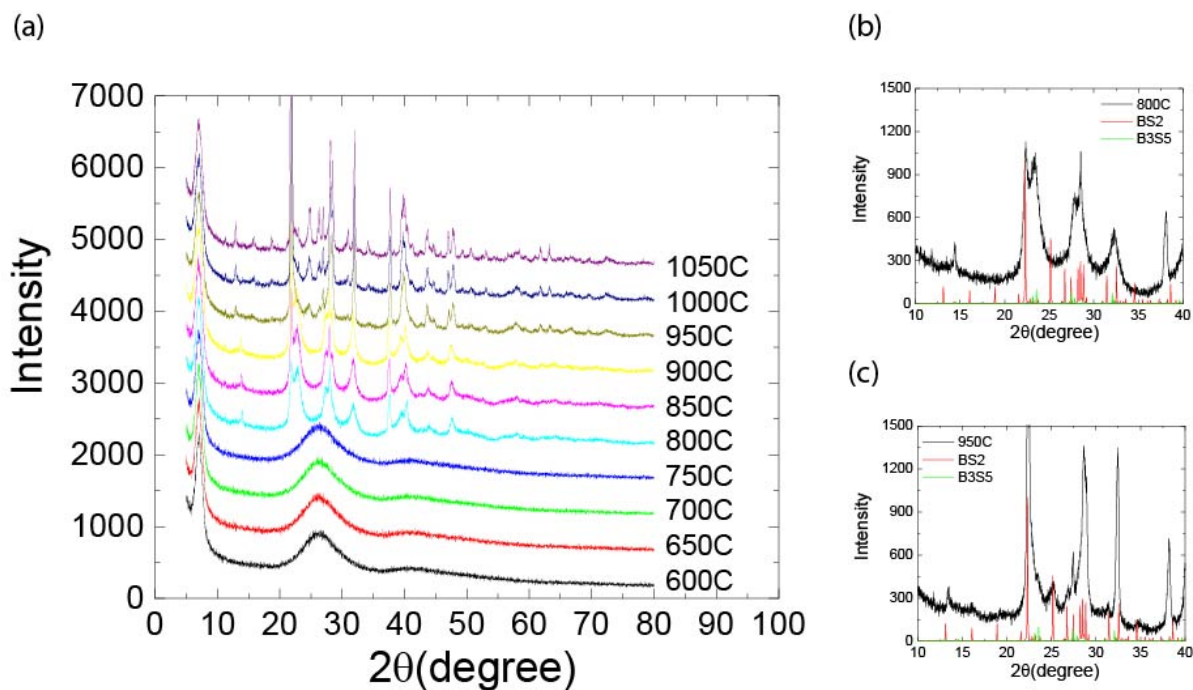


Figure 2. High temperature X-ray diffraction of barium disilicate glass. (a) Results of staircase temperature profile, with a 30 min hold at each temperature for data collection. Note the peak between 5 and 10° belongs to Kapton tape. (b) Comparison between 800°C data with BS2 and B3S5 profiles from the ICDD database, and (c) comparison between 950°C data with BS2 and B3S5 profiles from the ICDD database. In (b) and (c), constant 2-theta offset was applied to measured data to account for thermal expansion.

Based on these results, which provide general guidance on temperature and time necessary for initial crystallization, SEM analyses were used to define a narrower temperature range for the early stage nucleation process. Two barium disilicate glass samples, heat treated at either 735 or 780°C for two hours, were investigated by SEM and compared to the quenched glass. **Figure 3**, parts a and b, show the cross-section images of these samples. The quenched glass (i.e. no heat treatment)

and the 735°C/2h sample have identical amorphous morphologies, with no observable microstructure or inhomogeneities. The 780°C/2h sample showed a similar appearance to that of the other two, as can be seen in Figure 3c. However, upon closer examination, the SEM micrographs show a very low concentration of structural features, such as the one shown in **Figure 3d**. These features have a spherulitic shape and are a few micrometers in size, and the estimated volume fraction of these structures, based on SEM images, is much less than one percent. The morphology of the features is very similar to that reported in an earlier study [12] on high temperature crystallization in barium disilicate glass. Therefore, these features are believed to be associated with the early stage of crystallization and are consistent with crystallites detected by HTXRD around 800°C (**Figure 2a**).

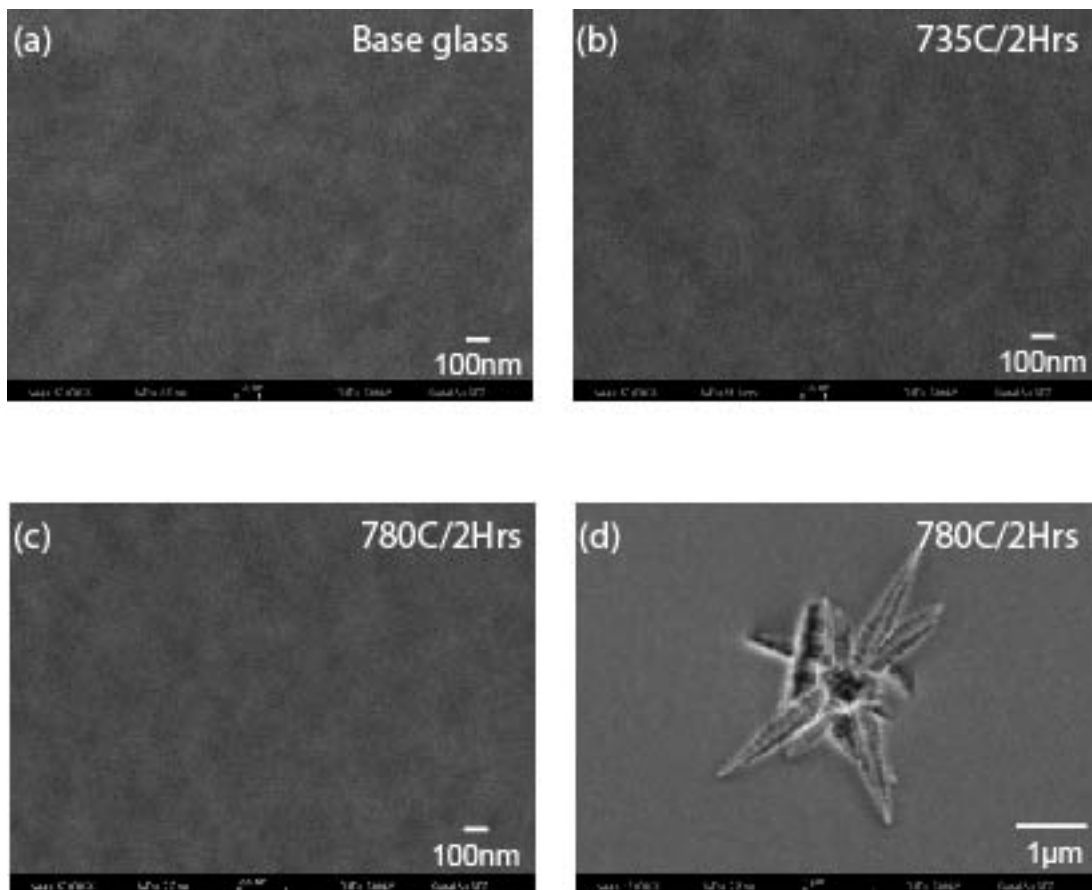


Figure 3 SEM of as-made (quenched) and heat-treated barium disilicate glass samples.

Images were taken on fractured cross sections after a 10 second 0.1% HF etch. (a) to (d) show the images of as-made glass, 735°C/2h, 780°C/2h, and large area scan for 780°C/2h, respectively.

These same heat-treated barium disilicate samples were then measured using ^{29}Si MAS NMR to investigate possible changes in local structure involving the silicon atoms. The ^{29}Si MAS NMR spectra of the 735°C/2h, 780°C/2h and quenched glass samples are plotted in **Figure 4**. The inset shows deconvolution of the glass data into three distinct peaks assigned to Q^2 , Q^3 and Q^4 silicate polyhedra. The relative concentrations of these Q^n species are consistent with the glass composition and results from prior NMR measurements of barium silicate glasses [29, 30]. Regarding the two heat-treated samples, the close similarity of the ^{29}Si NMR spectra with that of the quenched glass shows that there is no evidence of any significant change in the silicate network structure, indicating that these low temperature heat treatments did not induce changes in short-range structure as would occur if Si Q^n speciation were altered or if a sufficient portion of the silicate network became ordered via crystallization. These data are consistent with the SEM micrographs in indicating that there is no significant change in the average local chemical environment of the Si atoms, and likewise no detectable crystallization of the glass using this bulk spectroscopy. The volume fraction of the spherulites in the 780°C/2h sample (**Figure 3d**) must be quite small, with only a very limited number of such crystallites present throughout the sample.

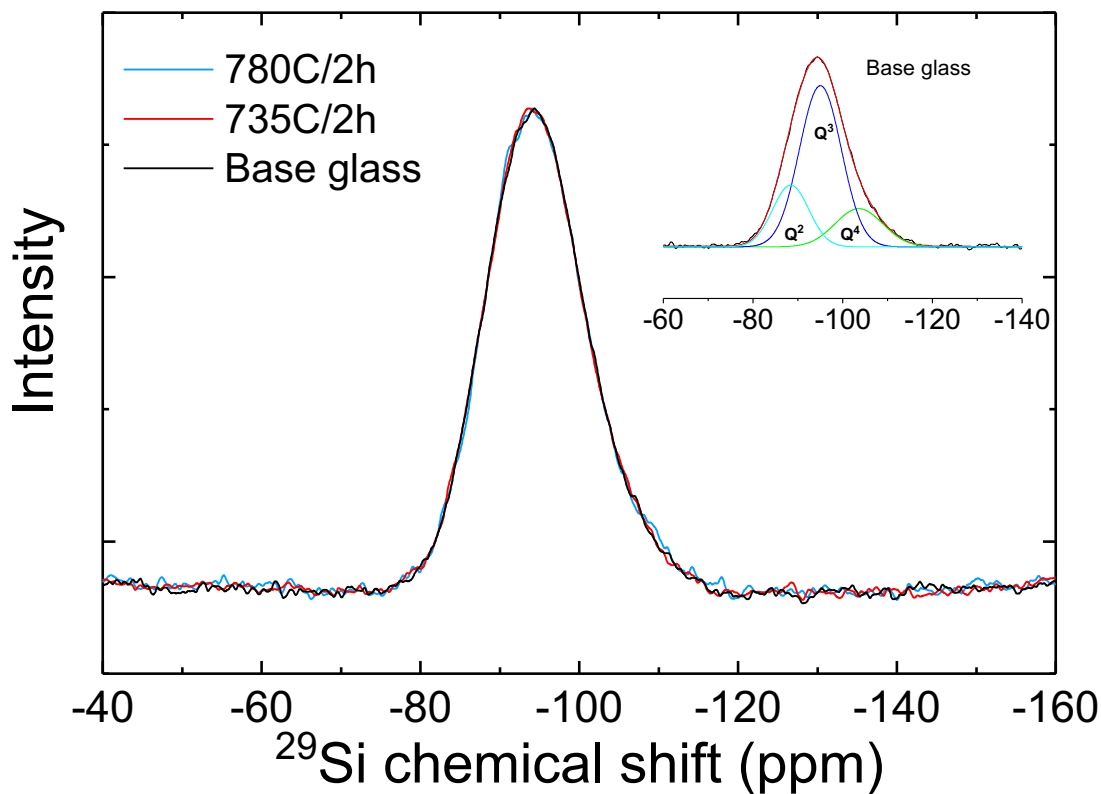


Figure 4 NMR of quenched and heat-treated barium disilicate glass samples. Black, red, and blue plots in the main figure represent base glass, 735°C/2h and 780°C/2h samples respectively. The inset shows the Q^n speciation of the quenched glass after deconvolution into three Gaussian peaks.

To further investigate the early stage nucleation, four barium disilicate glass samples were heat treated at a peak nucleation temperature of 725°C, as determined from previous studies [23, 9], for 5 h, 12 h, 30 h, and 40 h. The four samples are labeled as 725/5, 725/12, 725/30, and 725/40, respectively. Note that 725°C is close to the nucleation peak but well below the crystallization peak, T_{CR} . After the heat treatments, each of the four samples were first subjected to combined

USAXS/SAXS/WAXS ex-situ measurements. These data are presented in **Figure 5a-c**. In particular, the WAXS data show that there is no large-scale crystallization in any of the samples, although very weak diffraction peaks can be seen in the 725/40 sample at $Q = 2.26, 2.67,$ and 3.34 \AA^{-1} , see **Figure 5a**. Due to the similar d-spacing of the various BxSy crystalline phases, it is difficult to identify the phase assemblage exactly. However by comparing the approximate peak positions in **Figure 5a** and the calculated BxSy diffraction peaks in **Figure 5b**, the evidence strongly supports the presence of B3S5 and B5S8. The SAXS data in **Figure 5c** show very minimal changes for 725/5, 725/12, 725/30 samples. Only a small intensity increase can be observed in the 725/40 sample. Unlike the SAXS data, USAXS intensity increased significantly in the 725/30 sample, and even more so in the 725/40 sample, see **Figure 5d**. Since the WAXS measurement for the 725/30 sample shows no diffraction peaks, the USAXS data suggest very minor structural development already in the 725/30 sample, while the system remains on average amorphous.

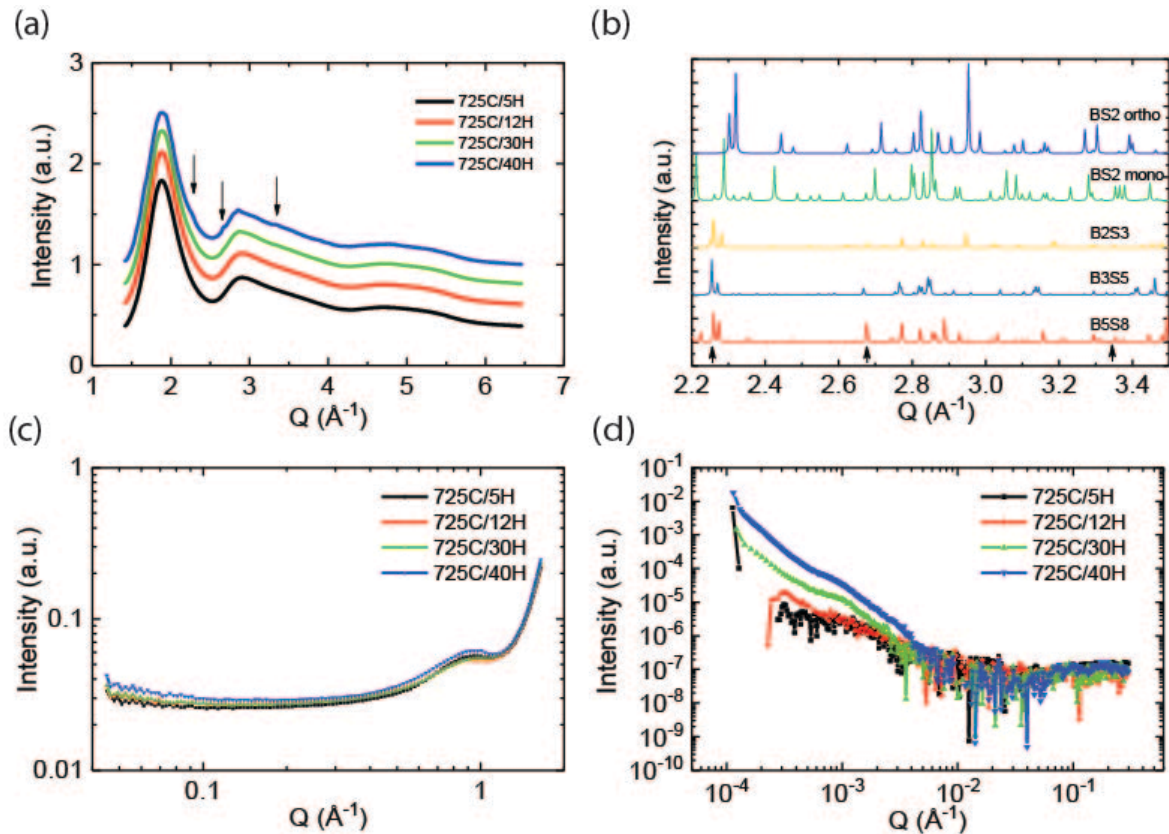


Figure 5 Barium disilicate glass samples heat treated at 725°C for 5 h, 12 h, 30 h and 40 h. (a)WAXS data indicate weak diffraction peaks only in the 40h sample, indicated by the arrows. (b) Calculated diffraction intensity of B_xS_y crystalline phase according to ICDD database. The arrows correspond to the approximate position of diffraction peaks in (a). SAXS and USAXS data are shown in (c) and (d) respectively.

These same samples were then analyzed by SEM to reveal the underlying structures. **Figure 6** shows the SEM images of these samples. The differences between the four samples are clearly observed. While the as-made glass does not show any microstructural heterogeneity, sub-micrometer sized spherical features appear early, after just 12 h. In the 30h and 40h heat-treated samples, these nano-structures grow both in number and size. Furthermore, a needle-like structure with $\sim 1\mu\text{m}$ size starts to develop in the 30h sample, and its number grows significantly in the 40h sample. However, it is not clear whether the needle-like features grow independently from the

spherulites or they form as a later-stage dendritic branch from the spherical core, since the spherical feature may be a cross-section perpendicular to the long-axis of a needle due to different orientations. Note that while the exact size of the nano-structures in the SEM image could be enhanced by etching during sample preparation, the resemblance of their morphology to that of high temperature crystallites formed after the 780°C/2h heat treatment suggests that they are crystalline.

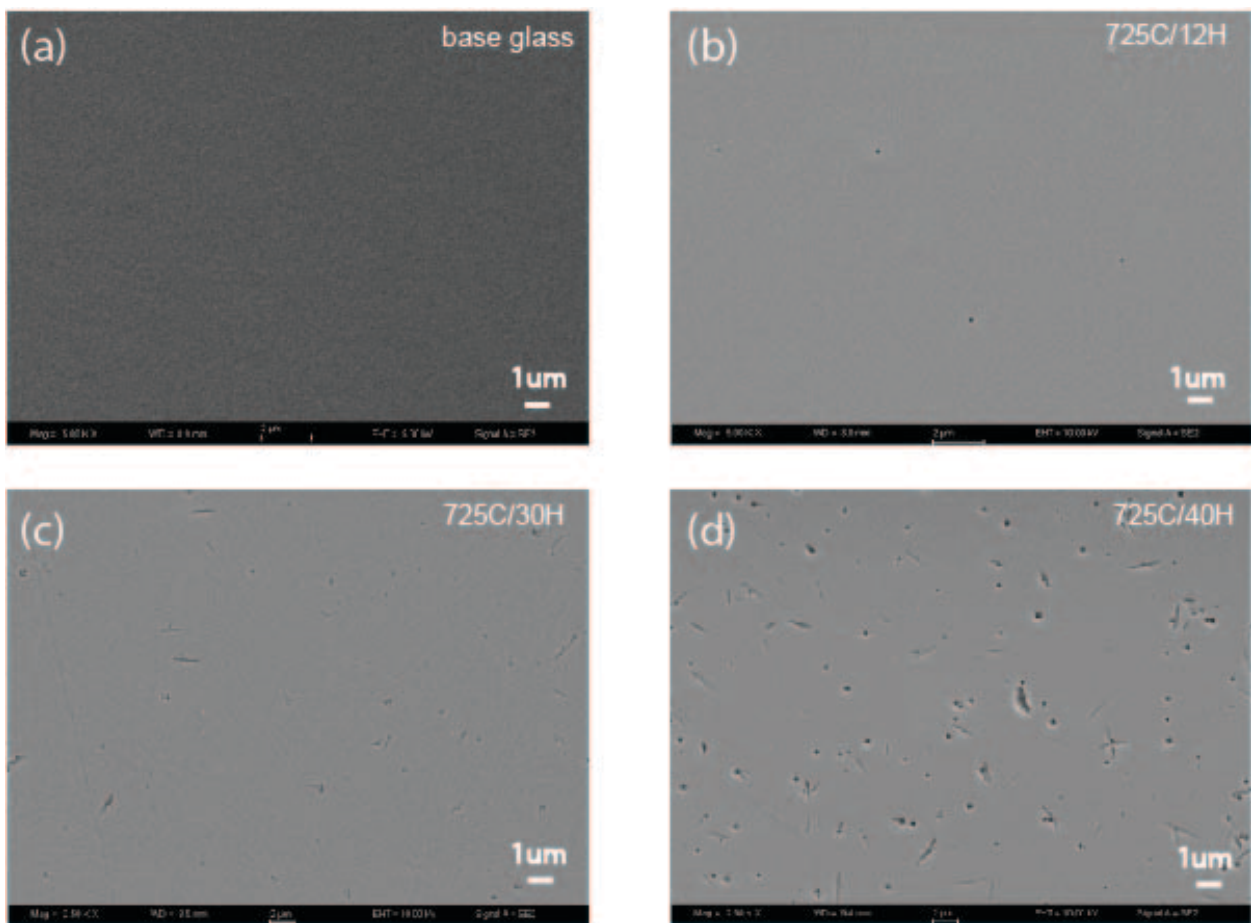


Figure 6 SEM images were taken for the same four samples after the USAXS/SAXS/WAXS measurements, (a) base (quenched) glass, (b)725°C/12h, (c) 725°C/30h, and (d)725°C/40h.

To investigate whether the nanostructures observed by SEM in the post-SAXS 725/30 sample are amorphous or crystalline in nature, the same samples were also analyzed by TEM. The structural analysis on both the needle-like and spherical regions showed ordered crystallinity, see **Figure 7**. In **Figure 7a**, a clear diffraction pattern is shown in the spherical region, indicating a non-amorphous nature. Note that the morphology of the spherulites revealed by SEM in the 725/30 sample is very similar to that of the 725/12 sample. The two images merely differ by the number density of these spherulites. Therefore, it is reasonable to believe that the non-amorphous nature of the spherulites in the 725/30 sample would also pertain to those in the 725/12 sample. The TEM diffraction pattern from the needle-like region also shows that they are crystalline in nature. As the atomic structure in the needle-like region appears to be highly ordered, an additional analysis was carried out to count Ba atoms which arrange in specific patterns that are unique to a certain BxSy stoichiometry at certain high-symmetry crystal zone axes (examples shown in **Figure 7**). The needle-like crystals have a dendritic structure, which is shown in the high-resolution STEM image in upper left inset in **Figure 7c**. The counted Ba atoms are labeled by the green circles [31]. The number of atoms can be matched to structures archived in the International Center for Diffraction Data (ICDD) database, see **Figure 7d-f**. B3S5 and B5S8 phases can be clearly identified in this region. However, due to the possible domain twinning in this region, the assignment of crystalline BS2 is unreliable.

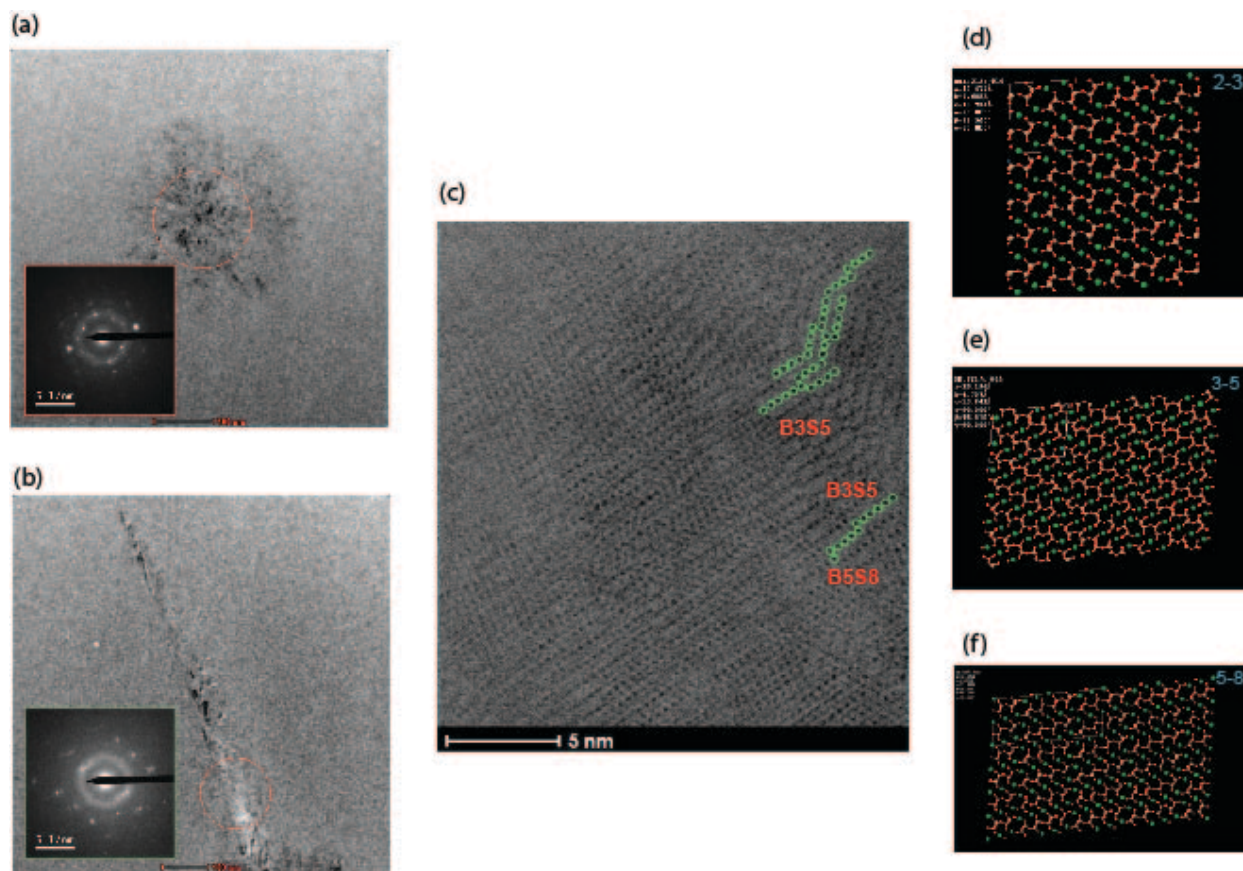


Figure 7 TEM analysis of the 725/30 barium disilicate sample. (a) and (b) TEM images and SAED patterns (inset) from the spherulite and needle-like regions, respectively. (c) High-resolution bright-field STEM image of the needle-like region. The green circles show the counting of Ba atoms with a zone-axis crystal orientation. These numbers can be matched to the barium silicate crystalline phase database to identify the B_xS_y stoichiometry. (d)-(g) show the atomic structure of barium silicate crystalline phases at certain high-symmetry orientations generated from the ICDD database. The green square in the inset image of figure (c) indicates the location from which the crystal lattice image was collected.

Another approach to understanding changes after 30 and 40h of isothermal treatment at 725°C is to evaluate the silicon speciation using ^{29}Si MAS NMR. Data for the same post-USAXS/SAXS/WAXS samples are plotted in **Figure 8**, and in comparison with the quenched glass spectrum in **Figure 4**, exhibit changes consistent with the nucleation behavior characterized above. Both post-SAXS samples show ^{29}Si NMR spectra which are narrower than that of the glass, indicating that the local silicate network has undergone some amount of ordering. There is

additional line narrowing on going from 30 to 40 hours of nucleation, as well as direct evidence for a small fraction of silicate groups in a crystalline environment, indicated by the sharp resonance around -90 ppm. The chemical shift of the new resonance is consistent with crystalline BS2 [30], though the range in ^{29}Si chemical shift is likely to be very small for the different BxSy phases since these all contain the same Q^n speciation. The NMR data in **Figure 8** also are consistent with differences between the 30 and 40h samples where, as shown by SEM images above, the latter contains a higher number of crystallites. It is only after 40h that a sufficiently large number of BxSy crystallites are present such that a bulk characterization technique like ^{29}Si NMR can detect them, though the exact nature of their structure cannot be ascertained by ^{29}Si NMR alone.

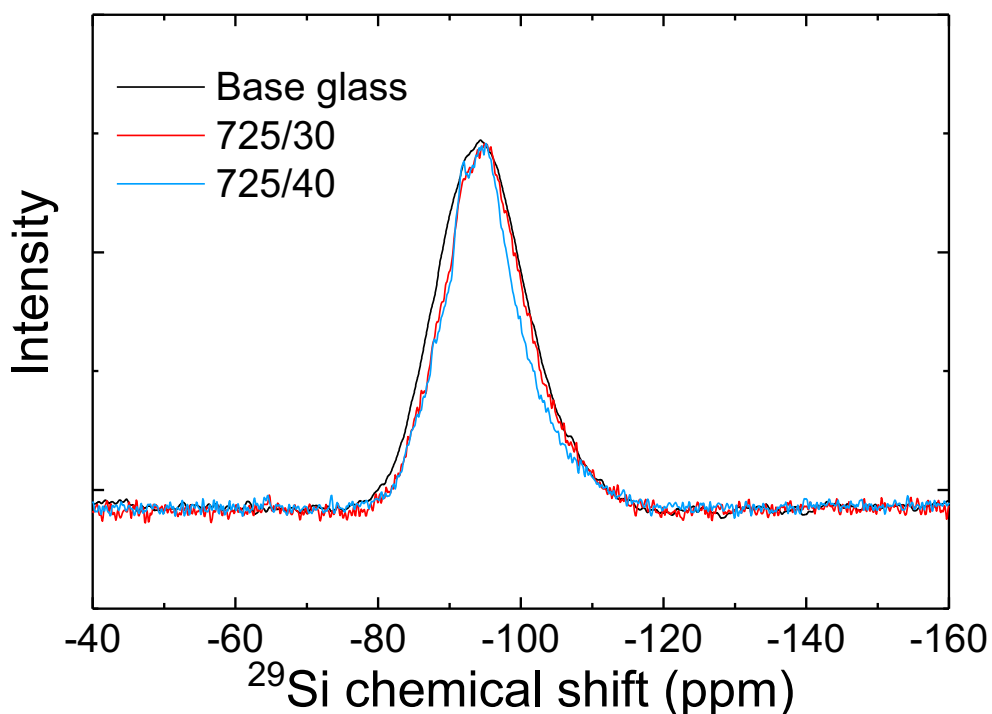


Figure 8 ^{29}Si MAS NMR spectra of quenched glass (black), 725/30 sample (red) and the 725/40 sample (blue).

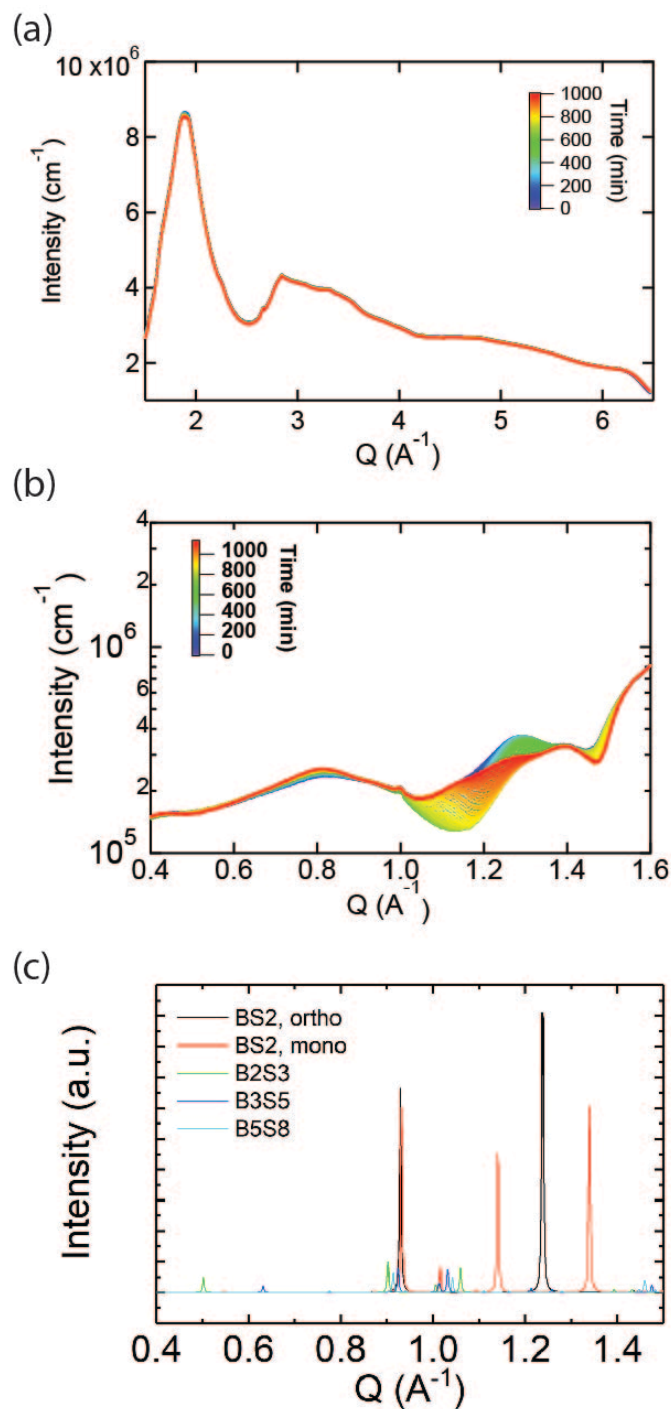


Figure 9 In-situ SAXS and WAXS of barium disilicate sample. The sample was heat treated at 725°C for 40 h prior to the measurement. Isothermal measurements were then performed at 725°C for 18 h. (a) Continuous WAXS data during the isothermal scan, and (b) continuous SAXS data during the isothermal scan. The color scale indicates time evolution. (c) Calculated diffraction intensity for BS2 (monoclinic and orthorhombic), B2S3, B3S5 and B5S8 phases.

The above presented WAXS, SEM, TEM, and NMR data indicate the presence of crystals in the 725/40 sample. To further investigate how this crystallinity developed in barium disilicate glass, the 725/40 sample was measured in-situ at the USAXS/SAXS/WAXS beamline for an additional 18 hours, held isothermally at 725°C. This sample was placed inside the Linkam heater and heated to 725°C at a rate of $\approx 200^\circ\text{C}/\text{min}$. The SAXS/WAXS data were collected continuously for ~ 18 hours. As the sample had already been heat-treated for 40-hours, the in-situ data represent the 40 to 58-hour period of the nucleation process at 725°C. **Figure 9a** and **b** show the continuous scan of WAXS and SAXS data, respectively. The color scale represents the time evolution during the isothermal scan. The intensity without significant color change suggests no structural change during the isothermal hold. On the other hand, if the intensity changes with time during the isothermal hold, the underlying structures with corresponding q -range are evolving with time. The WAXS data show negligible change in diffraction intensity during the 18-hour measurement, indicating that the average volume fraction of crystalline phase remained unchanged. However, in high- Q SAXS data, there is significant change of intensity during the 18-hour measurement. Between $Q = 1 \text{ \AA}^{-1}$ and 1.4 \AA^{-1} in **Figure 9b**, two regions of intensity changed distinctively. The intensity near $Q = 1.15 \text{ \AA}^{-1}$ decreased for the first 12 hours, then it started to increase between 12 and 18 hours, whereas the intensity near $Q = 1.3 \text{ \AA}^{-1}$ decreased continuously for the first 18 hours. In **Figure 9c**, calculated intensities for BS2, B2S3, BS2, B3S5, and B5S8 diffraction peaks are presented. BS2 is the strongest scattering phase in this Q -region, and between $Q = 1$ and 1.4 \AA^{-1} BS2 is the only visible phase that shows any diffraction peaks. Therefore, the structural changes during the isothermal hold could be related to precursors of the BS2 crystalline phase. While there is no clear explanation for the amorphous structural change at the specific Q values, the apparent connection between the changing intensity in the in-situ SAXS measurement and the calculated diffraction pattern is further discussed below.

IV. DISCUSSION

Many pioneering studies on the barium disilicate system have attributed its nucleation to a homogeneous process due to the formation of predominantly BS2 crystalline phase after the growth stage [8, 14, 26]. In contrast to these early findings, our experimental evidence suggests that the nucleation in barium disilicate glass exhibits a more inhomogeneous nature, namely BxSy phases with Ba/Si >0.5 appear at the early stage of nucleation concurrently with, if not prior to, the BS2 crystalline phase [14, 26]. Such a finding is similar to that reported by Takahashi et al., where higher ratio Ba/Si phases were found in a barium disilicate sample heat treated at 775°C [17]. In this study we further lowered the temperature to investigate the structural changes and crystallinity at the initial stage of nucleation. Most of the analyses were carried out around heat treatment at 725°C, where no structural changes were observed in DSC and in-situ XRD measurements. Ex-situ measurement by SEM and NMR also indicated no change in Si coordination or microstructure development after the 725/2 treatment. These findings indicate that 725°C is clearly below any significant crystal growth temperature. Prolonged heat treatment at 725°C revealed that structural changes can develop in the glass matrix after a 30-hour treatment at this temperature, see **Figure 5c**. An extremely low volume fraction of spherulite phase can be found in an SEM image of the 725/12 sample. Only after 40 hours of heat treatment at 725°C can weak diffraction peaks be measured (see **Figure 5a**), and peak position suggest a mixed phase assemblage at the initial stage. The change of structure after 30 and 40 hour heat treatments was further corroborated by ²⁹Si NMR data for the same samples that had previously undergone USAXS/SAXS/WAXS measurements, in which the ²⁹Si resonance in the 725/30 sample is consistent with silica network ordering, and furthermore, in the 725/40 sample, spectral changes are consistent with barium silicate crystalline phase formation.

The most striking evidence for the appearance of B_xS_y phases with Ba/Si>0.5 at early stages of nucleation comes from the TEM image analysis, where B₃S₅ and B₅S₈ phases are found in the high-resolution bright-field STEM image of the needle-like region in the 725/30 sample. Because of the similar ordering as the BS₂ phase, these higher Ba/Si ratio phases are difficult to identify in diffraction measurements. However, high resolution STEM images allow us to identify these phases by directly counting the number of Ba atoms along high symmetry direction, where they are arranged in rows with different numbers of atoms characteristic of certain stoichiometries. The TEM analysis clearly shows that (1) the nanostructures that appear in the early stage of nucleation are already crystalline, and (2) the initial phases include B₃S₅ and B₅S₈. It should also be mentioned that neither diffraction nor lattice imaging allowed us to identify the crystal phase in the “trunk” region of needle-like crystals. This is because crystal orientation by TEM stage tilting was prohibitive due to extended exposure resulting in amorphization (electron beam damage) of these features. Alternatively, the trunk could be partially disordered. There are two reasons to suspect this from the TEM data perspective: 1) only a small portion of the trunk in the analyzed needle-like crystal was apparently crystalline and appeared as a dark patch in the low-magnification image of the needle; 2) significantly brighter contrast of the trunk compared to the crystalline branches in bright-field TEM images indicating relatively lower diffraction intensity, which can be because the crystals in the trunk are far from any zone axis or because it is disordered.

To understand the origin of the inhomogeneous nucleation, simulated XRD patterns of all the barium silicate phases available in the ICDD database were plotted. **Figure 9c** shows the calculated intensity for BS₂ (monoclinic and orthorhombic), B₂S₃, B₃S₅, and B₅S₈ phases. It is interesting to note that, while no diffraction peaks appear in the WAXS data, the intensity between $Q = 1 \text{ \AA}^{-1}$ and 1.4 \AA^{-1} in SAXS data showed strong time dependent evolution. It is clear that the signal

intensity decreased for the first 10 hours, and then started to rise again. Since this Q-range corresponds to BS2 lattice spacing, the initial decrease of intensity in this region seems to suggest that the early stage crystalline phase is not BS2. Note that a similar observation was also discussed by Moulton et al. using the argument of preferred topology of B2S3, B3S5 and B5S8 in the supercooled state [16]. Based on the in-situ SAXS findings, it is tempting to attribute the initial formation of higher Ba/Si phases to the depletion of Ba atoms from the glass matrix. Although the true origin of the higher Ba/Si phases in the early stage needs further understanding, an increasing amount of evidence has shown that the barium disilicate glass does not transform directly into the BS2 crystalline phase at the early stage, which suggests an inhomogeneous nucleation nature.

Not only do the above data provide insight into the crystallinity of the nano-structures in the early growth stage, they also shed light on the immiscibility of barium disilicate glass in the supercooled liquid state. Earlier studies offered speculation on whether barium disilicate would nucleate and subsequently crystallize without undergoing liquid/liquid phase separation [10, 8, 28]. In our study, the results from SEM, NMR and SAXS indicate there is no phase separation in as-made glass, or in 735/2 and 725/5 heat treated samples. The prolonged 725°C heat treatment leads to the growth of observable nano-structures while the sample remains on average amorphous, e.g. SEM images of 725/12 and 725/30 samples confirming crystalline domains, while the bulk of the Si speciation is amorphous as detected using ²⁹Si MAS NMR. However, TEM analysis of the 725/30 sample clearly indicates arrangement of nanocrystals into the dendritic structure in the “branches” of the needle like particles, and in the spherulitic particles. TEM analysis was not performed on the 725/12 sample because of the extremely low volume fraction of these nano-structures. However, the remarkably similar morphology of the 725/12 sample and those treated at longer times leads us to believe that some crystallinity already formed in the 725/12 sample. Because crystallinity is found in such an

early stage of these isothermal heat treatments, it is highly likely that the nucleation process begins without going through the liquid/liquid phase separation stage.

V. CONCLUSION

The comprehensive experimental investigation presented in this work sheds light on the complex nucleation process in the barium disilicate system. The data clarify earlier speculation on how the barium disilicate system is differentiated from the other barium silicate systems with higher or lower Ba/Si ratio. In particular, the combined TEM and SAXS data revealed that sub-micrometer sized crystallites grow out of the glass matrix without any evidence for a preceding liquid-liquid phase-separation. In addition, our data show clear evidence for the nucleation mechanism of barium disilicate glass when heated above the glass transition temperature. Although BS2 is the final phase once the system is fully crystallized, the initial crystallites more likely contain B3S5 and B5S8, which is consistent with an inhomogeneous nucleation process. This is a new finding since the system was previously believed to congruently transform from barium disilicate glass to BS2 crystalline phase, and this understanding may shed light on nucleation processes in other glasses.

ACKNOWLEDGMENTS

The authors would like to thank Dr. Jan Ilavsky for helping with the SAXS experiment and Mike P. Carson for sample preparation. We are also very grateful for Prof. Ken Kelton and Dr. Richard Weber for many fruitful discussions. Use of the Advanced Photon Source, an Office of Science

User Facility operated for the U.S. Department of Energy (DOE) Office of Science by Argonne National Laboratory, was supported by the U.S. DOE under Contract No. DE-AC02-06CH11357

Bibliography

- [1] S. G. Lu, C. L. Mak, and K. H. Wong, "Optical studies of transparent ferroelectric strontium–barium niobate/silica nanocomposite," *J. of Appl. Phys.*, vol. 94, p. 3422, 2003.
- [2] K. Shinozaki, T. Honma and T. Komatsu, "Morphology and dispersion state of Ba₂TiSi₂O₈ nanocrystals in transparent glass-ceramics and their nanoindentation behavior," *J. of Non-Cryst. Solids*, vol. 358, p. 1863, 2012.
- [3] N. F. Borrelli and M. M. Layton, "Dielectric and optical properties of transparent ferroelectric glass-ceramic systems," *J. of Non-Cryst. Solids*, vol. 6, p. 197, 1971.
- [4] W. Hölland and G. H. Beall, *Glass-ceramic technology*, Wiley, 2002.
- [5] Q. Fu, G. H. Beall, and C. M. Smith, "Nature-inspired design of strong, tough glass-ceramics," *MRS Bulletin*, vol. 42, no. 3, p. 220, 2017.
- [6] E. D. Zanotto, "A bright future for glass-ceramics," *American Ceramic Society Bulletin*, vol. 89, no. 8, 2010.
- [7] H. Jain, "Transparent Ferroelectric Glass-Ceramics," *Ferroelectrics*, vol. 306, p. 111, 2004.
- [8] T. P. Seward, D. R. Uhlmann and D. Turnbull, "Development of Two-Phase Structure in Glasses, with Special Reference to the System BaO-SiO₂," *J. of Am. Ceram. Soc.*, vol. 51, no. 11, p. 634, 1968.
- [9] A. H. Ramsden and P. F. James, "The effects of amorphous phase separation on crystal nucleation kinetics in BaO-SiO₂ glasses, Part 1: General survey," *J. of Mat. Sci.*, vol. 19, p. 1406, 1984.
- [10] A. H. Ramsden and P. F. James, "The effects of amorphous phase separation on crystal nucleation kinetics in BaO-SiO₂ glasses, Part 2: Isothermal heat treatments at 700°C," *J. of Mat. Sci.*, vol. 19, p. 2894, 1984.
- [11] E. D. Zanotto, P. F. James, and A. F. Craievich, "The effects of amorphous phase separation on crystal nucleation kinetics in BaO-SiO₂ glasses, Part 3: Isothermal treatments at 718 to 760°C; small-angle X-ray scattering results," *J. of Mat. Sci.*, vol. 21, p. 3050, 1986.
- [12] J. F. MacDowell, "Nucleation and Crystallization of Barium Silicate Glasses," *Proc. of Bri. Ceram. Soc.*, vol. 3, p. 101, 1965.
- [13] H. Hasegawa and I. Yasui, "X-ray and neutron diffraction analyses of barium silicate glass," *J. of Non-Cryst. Solids*, vol. 95, p. 201, 1987.
- [14] E. D. Zanotto and P. F. James, "Experimental test of the general theory of transformation kinetics: Homogeneous nucleation in a BaO · 2SiO₂ glass," *J. of Non-Cryst. Solids*, vol. 104, p. 70, 1988.
- [15] L. A. Silva, J. M. R. Mercury, A. A. Cabral, "Determining the Crystal Volume Fraction of

- BS2 Glass by Differential Scanning Calorimetry and Optical Microscopy," *J. of Am. Ceram. Soc.*, vol. 96, p. 130, 2013.
- [16] B. J. A. Moulton, A. M. Rodrigues, D. V. Sampaio, L. D. Silva, T. R. Cunha, E. D. Zanotto and P. S. Pizani, "The origin of the unusual DSC peaks of supercooled barium disilicate liquid," *Cryst. Eng. Comm.*, vol. 21, p. 2768, 2019.
- [17] Y. Takahashi, M. Osada, H. Masai, and T. Fujiwara, "Transmission electron microscopy and in situ Raman studies of glassy sanbornite: An insight into nucleation trend and its relation to structural variation," *J. of Appl. Phys.*, vol. 108, p. 063507, 2010.
- [18] Y. Takahashi, M. Osada, H. Masai, and T. Fujiwara, "Structural heterogeneity and homogeneous nucleation of 1BaO-2SiO₂ glass," *Appl. Phys. Lett.*, vol. 94, p. 211907, 2009.
- [19] M. C. C. Araujo, W. J. Botta, M. J. Kaufmann, R. S. Angelica, J. M. R. Mercury, A. A. Cabral, "Residual glass and crystalline phases in a barium disilicate glass-ceramic," *Materials Characterization*, vol. 110, p. 192, 2015.
- [20] M. E. McKenzie, S. Goyal, T. Loeffler, L. Cai, I. Dutta, D. E. Baker, and J. C. Mauro, "Implicit glass model for simulation of crystal nucleation for glass-ceramics," *npj Comp. Mat.*, vol. 4, p. 59, 2018.
- [21] Massiot, D. and Fayon, F. and Capron, M. and King, I. and Le Calve, S. and Alonso, B. and Durand, J.O. and Bujoli, B. and Gan, Z. and Hoatson, G., "Modelling one- and two-dimensional solid-state NMR spectra," *Magnetic Resonance in Chemistry*, vol. 40, pp. 70-76, 2002.
- [22] J. Ilavsky, F. Zhang, R. N. Andrews, I. Kuzmenko, P. R. Jemian, L. E. Levine, A. J. Allen, "Development of combined microstructure and structure characterization facility for in situ and operando studies at the Advanced Photon Source," *J. of Appl. Cryst.*, vol. 51, p. 867, 2018.
- [23] X. Xia, I. Dutta, J. C. Mauro, B. G. Aitken, K.F. Kelton,, "Temperature dependence of crystal nucleation in BaO·2SiO₂ and 5BaO·8SiO₂ glasses using differential thermal analysis," *J. of Non-Cryst. Solids*, vol. 459, p. 45, 2017.
- [24] G. OEHLSCHEGEL, "Crystallization of Glasses in the System BaO·2SiO₂-2BaO·3SiO₂," *Journal of The American Ceramic Society*, vol. 58, p. 148, 1975.
- [25] H. Tanigawa and H. Tanaka, "Crystallization of Some Glasses in the BaO-SiO₂ System," *Osaka Kogyo Gijutsu Shikensho kiho*, vol. 18, no. 3, p. 230, 1967.
- [26] B. J. A. Moulton, A. M. Rodrigues, P. S. Pizani, D. V. Sampaio, E. D. Zanotto, "A Raman investigation of the structural evolution of supercooled liquid barium disilicate during crystallization," *Int. J. of Appl. Gla. Sci.*, vol. 9, p. 510, 2018.
- [27] K.F. Hesse and F. Liebau, "Crystal chemistry of silica-rich Barium silicates III: Refinement of the crystal structures of the layer silicates Ba₂(Si₄O₁₀) (I), (Sanbornite), and Ba₂(Si₄O₁₀) (h)," *Z. Kristallogr.*, vol. 33, p. 153, 1980.
- [28] W. Haller, D. H. Blackburn, and J. H. Simmons, "Miscibility Gaps in Alkali-Silicate Binaries—Data and Thermodynamic Interpretation," *J. of Am. Ceram. Soc.*, vol. 57, p. 120, 1974.
- [29] J. Schneider, V.R. Mastelaro, E.D. Zanotto, B.A. Shakhmatkin, N.M. Vedishcheva, A.C. Wright and H. Panepucci, "Qn distribution in stoichiometric silicate glasses: thermodynamic calculations and ²⁹Si high resolution NMR measurements," *J of Non-Cryst. Solids*, vol. 325, 2003.
- [30] J.B. Murdoch, J.F. Stebbins and I.S.E. Carmichael, "High-resolution ²⁹Si NMR study of silicate and aluminosilicate glasses: the effect of network-modifying cations," *American Mineralogist*, vol. 70, p. 332, 1985.

- [31] M. Czank, P. R. Buseck, "Crystal chemistry of silica-rich barium silicates," *Z. Kristallogr. Cryst. Mater*, vol. 153, pp. 19-32, 1980.
- [32] J. Deubener, M. Montazerian, S. Krüger, O. Peitl, E. D. Zanotto, "Heating rate effects in time-dependent homogeneous nucleation in glasses," *J. of Non-Cryst. Solids*, vol. 474, p. 1, 2017.
- [33] H. E. Swanson, H. F. McMurdie, M. C. Morris, and E. H. Evans, "Standard X-ray Diffraction Powder Patterns," in *Natl. Bur. Stand. (U. S.) Monogr.* , vol. 25, Washington, D.C., 1970, pp. 1-171.